Analysis of Pressure Drop Data in Channel Flows Over Foul-Control Coatings

ANALYSIS OF PRESSURE DROP DATA IN CHANNEL FLOWS OVER FOUL CONTROL COATINGS

Irma Yeginbayeva, Chalmers University of Technology, Gothenburg, Sweden
Valery Chernoray, Chalmers University of Technology, Gothenburg, Sweden
Lena Granhag, Chalmers University of Technology, Gothenburg, Sweden

The two-dimensional channel flow is of great interest for experimental as well as numerical studies. From the experimental perspective test in channel equipment is preferred, because it is simple, practical and offers a favorable economic running cost. Especially with the growing interest in marine coating research, it is critical that coating testing equipment delivers realistic flow conditions, is simple to cut the experimental time and effort and yet accurate. In this sense, the flow channel facility offers more advantages than classical cases for experimental investigations. Whereas from the numerical investigations point of view, channel flow exhibits favorable boundary conditions to save computational effort, while providing a deep insight into details of the flow structures. An initiative is taken at Chalmers university to develop the channel flow (or a flowcell) experimental facility to cater for the need of studies on coatings. Therefore, the current paper, in the first step, describes the design and manufacture of the flowcell. Secondly, it presents the thoroughly conducted verification study of the smooth reference test section to demonstrate that experimental facility holds the measurement expectations. Subsequently, skin friction data for selected foul control coatings obtained from the pressure drop measurements in the flowcell are presented.
Keywords Pressure drop, channel flow, marine commercial coatings, Skin frictional drag

1. Introduction

An ideal channel flow is defined as the steady flow between two parallel plates of a certain distance, *H*. Due to infinite length and width of panels, the flow is considered as two-dimensional. Therefore, following simplified assumptions are made when building such channel flow device and validating experiments: a) the two-dimensionality of the flow; b) a fully developed flow in the test section; c) installed parallel walls (or panels) do not leave gaps/steps in the measuring section. While the full development of flow in the channel can be ensured by having an adequate length of the channel, the perfect two-dimensionality of the flow can only be achieved in theory, since it is easy and possible to make assumptions about the infinite plate length and width. However, in reality, this is not practical and nearly impossible. Hence, in experimental studies of channel flows the sufficient ratio between channel width (*W*) and height (*H*) in order to avoid three-dimensional effects has been questioned and argued by numerous studies[1], [2], [3]. Dean [4] after comprehensive literature survey suggested an aspect ratio, AR of 7 (AR=width divided by the channel height=W/H). Schultz and Flack [5] carried out experiments in high Reynolds number turbulent channel flow with an AR of 8 and found similar Reynolds number scaling trends with experimental results from pipe and boundary layer flows. According to Zanoun [6] and Monty [2], the ARs of 11.7-12 are sufficient to maintain nominally two-dimensional flow conditions. Vinuesa *et al* [3] carried out experiments in a variable AR duct flow facility with the aim to study the flow development and skin friction dependence on the duct AR, which was varied from 12.1 to 48. The first conclusion of this study was that two-dimensional turbulent channel flows cannot be reproduced experimentally. According to Vinuesa *et al*, skin friction becomes independent of AR at ratios 24 and higher, and flow becomes truly fully developed for development length, *x/H* values larger than 200. As can be noticed, both are nearly double what was previously thought sufficient for channel flows. It is worth to mention here, that experimental

and numerical studies on high AR and longer channel lengths are rare. Vinuesa *et al* [3] also noticed that for high Reynolds numbers, smaller values of *x/H* such as 120 may be adequate.
Dean [4] collected many data from different investigators (27 sources from 1928 to 1976) for hydraulically smooth channel flows. This data was used to illustrate all sources in one diagram as change of skin friction coefficient with Reynolds number. Based on this dataset, Dean develop his correlation for friction factor in (1.

$$C_f = 0.073 {Re_m}^{-0.25} \quad (1)$$

Dean's curve is widely accepted and numerous study results ([7], [8], [2], [5]) are in the vicinity of this correlation. For representation of wall skin friction data, Zanoun, Durst [6] suggested a slightly modified equation, which is:

$$C_f = 0.058 {Re_m}^{-0.243} \quad (2)$$

To cater for the need of studies on coatings, an initiative was taken at Chalmers university to develop the channel flow (or flowcell) experimental facility. This paper introduces the flowcell that has been designed and built within the project. The paper is divided to three main parts. The Section 1 establishes the concept for channel flows, whereas the Section 2 provides a detailed description of the facility, which was built based upon concepts in Section 1. In order to verify that the flowcell holds the desired performance, the pressure drop and mass flowrate must be measured. Therefore, Section 3 describes details of main measurements. Subsequent Section 4 lists all surfaces tested as part of the experimental campaign. Finally, Section 5 focuses on the capabilities of the set-up by demonstrating achievable velocities in the testing section and grading of different surfaces according to obtained skin friction curves. Hence the objectives of this investigation can be formulated as follows: a) to present friction data on smooth channel of rectangular cross section, to discuss this data and to compare it with previous work of a similar nature; b) to demonstrate the capability of set up in comparison to previously collected results for various types of reference and foul control coatings.

2. Description of the Flowcell

The flowcell equipment was designed at Chalmers university with the main aim to measure the skin friction for coated panels under turbulent flows. The flowcell as demonstrated in Figure 1a**Error! Reference source not found.**, is a closed test chamber composed of pipe bends, contraction (entry part), flow development section (acrylic part), pressure drop measuring part (with red panel on) and outlet or diffuser (end part). This equipment was designed to utilize a flat polyvinyl chloride (PVC) or polymethyl methacrylate (PMMA) panel with a length, width and thickness of $280-0.2$mm, 95 ± 0.2mm and 5 ± 0.2mm, respectively as demonstrated in Figure 2. The development length is *x/H*=70. This is in accordance with Durst [1], who recommends *x/H*=60. From an asymptotic approach a development length of *x/H*=25 is indicated to be sufficient in a channel [9]. According to Zanoun, Nagib [8], a development length of *x/H*=30 was sufficient to ensure a fully developed state of the mean pressure distribution in the flow direction. For a turbulent flow commonly the development length is recommended to be independent of the Reynolds number. The pressure drop/measuring section have a cross sectional area of 10mm x 80 mm. Here, a 10mm corresponds to distance between two parallel flat panels and 80mm is equivalent to the wetted panel's width. The flowcell has the AR of 8, which was found as an appropriate compromise based on the recommendations in the literature.

Figure 1. a) The flowcell overview; b) Installation of coated test panel (red) in the testing section

Handling of a test section in case of exchanging test panels forming side walls is relatively easy. To enable replacement, these panels are pressed on a grove that controls a 10mm channel height and supported by plastic plates which are screwed to the main PVC frame (see Figure 1b). Pressure taps were installed at the top or in the middle of two parallel panels at 15mm distance away from leading and trailing edge of the test panels. The distance between the taps is 250mm, which covers almost 90% length of the inserted panels. The readings of transducer from pressure taps were used to evaluate the differential pressure change over reference and different coated panels. The flowcell is driven by *Grundfos USP Series 200* pump by a variable frequency inverter to control the speed of standard 3-

phase induction motor. The pump has the capacity of 40-45 m^3/hour. All the components of the facility are corrosion resistant and exhibit minimal metal ion release into the recirculating system.

Figure 2. Two hydraulically smooth PVC plates for side walls forming a channel with width and height of 80mm and 10mm respectively corresponding to AR=8

3. Testing procedure

3.1 Flowrate measurements

To establish the mean velocities (U_m), thus the Reynolds number (Re_m) in the test section for each corresponding pump frequencies, flowrate measurements were conducted in the system with the help of venturi meter. Venturi meter is a flow measurement instrument, which use a converging section of pipe to give the pressure drop from which the flowrate can be deduced. In this study, venturi tube was designed as shown in Figure 3a and 3D printed to be fitted just before the contraction section at the channel entry. The venturi design follows ASME recommendations. Figure 3b presents the 3D printed flowmeter based on venturi effect with integrated pressure taps. These pressure taps were installed to measure a pressure difference of the fluid at the two sections, first at the inlet (Section 1) and the second one is at the throat (Section 2). At the section 1, the pressure of the fluid is maximum and the velocity is minimum. Whereas at the section 2, the velocity of the fluid is maximum and the pressure is minimum (see Figure 3a). The pressure difference at the two sections was recorded via differential pressure transducer attached to sections. The difference in the pressure heads of these two sections is used to calculate the rate of flow through venturi meter. In the current study, pipe diameters for the section 1 (high pressure) and the section 2 (low pressure) were 46 mm and 34 mm, respectively.

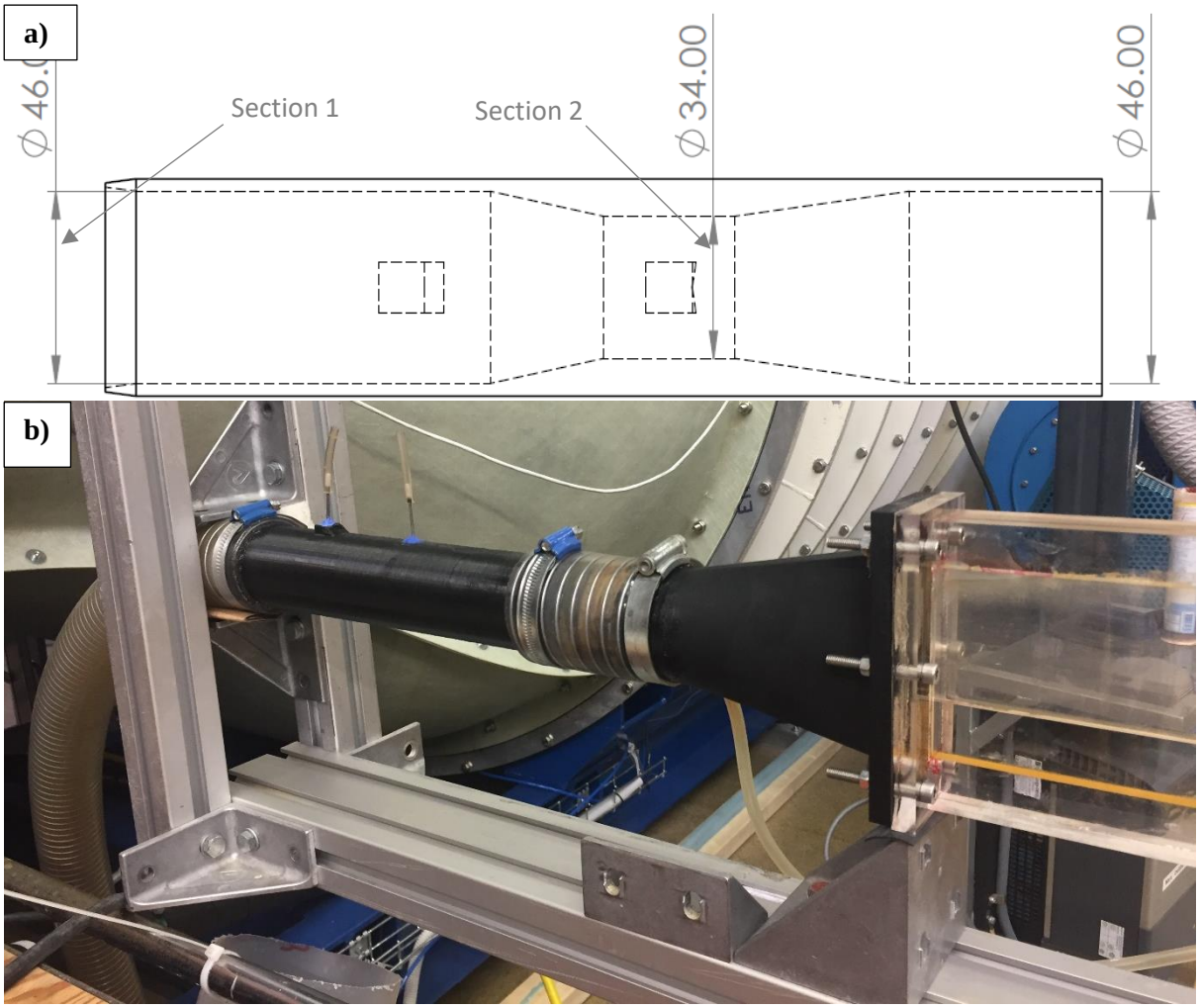

Figure 3. a) Drawing of Venturi tube; b) 3D printed Venturi tube installed upstream of the channel's contraction inlet

The pressure differences across the venturi tube were measured. If an incompressible flow through the venturi tube is considered and Bernoulli's theorem is applied to the flow crossing the upstream (Section 1) and the throat section (Section 2), then the following equation will be given for the flow:

$$p_1 + \frac{1}{2}\rho {u_1}^2 = p_2 + \frac{1}{2}\rho {u_2}^2 \quad (3)$$

Where p, ρ and u are the pressure, fluid density and mean velocity. The superscripts 1, 2 refer to upstream and throat sections.
Conservation of mass gives:

$$Q = \frac{1}{4}\pi D^2 u_1 = \frac{1}{4}\pi d^2 u_2 \quad (4)$$

Where Q is volumetric flowrate, D and d are the upstream and throat pipe diameters.
Combining (3 and (4:

$$Q = C\frac{\pi d^2}{4}\frac{1}{\sqrt{(1-ß^4)}}\sqrt{\frac{2(p_1-p_2)}{\rho}} \quad (5)$$

Where ß is the diameter ratio, $\frac{d}{D}$. To account for small pressure losses, the equation is multiplied by the discharge coefficient, C [10]. Discharge coefficient for current venturi meter was found to be 0.8 [11]. Knowing the flowrate and cross-sectional area of the test section enabled the recalculation of volumetric flowrate at different pump frequencies in terms of mean velocities (See section 5.1).

3.2 Estimation of skin friction coefficient from pressure drop measurements

A high accuracy USB output pressure transducer (*X409 USBH*) from *Omega Engineering, Inc* (Norwalk, CT, USA) was used to measure pressure drop over test panels and in venturi tube. Transducer connects directly to a PC. Dedicated *Omega* software was utilized as a virtual meter, chart recorder, or data logger. This sensor provides a very stable transducer with an exceptional high accuracy of ±0.08% and a broad compensated range of -29°C to 85°C (-20°F to 185°F). During data logging and at each pump frequency changes, the measurement curve was constantly observed (see Figure 4a). A minimum of 30 sec of pressure readings were collected when the flow fully developed and reached the steady state at given flow condition (Figure 4b).

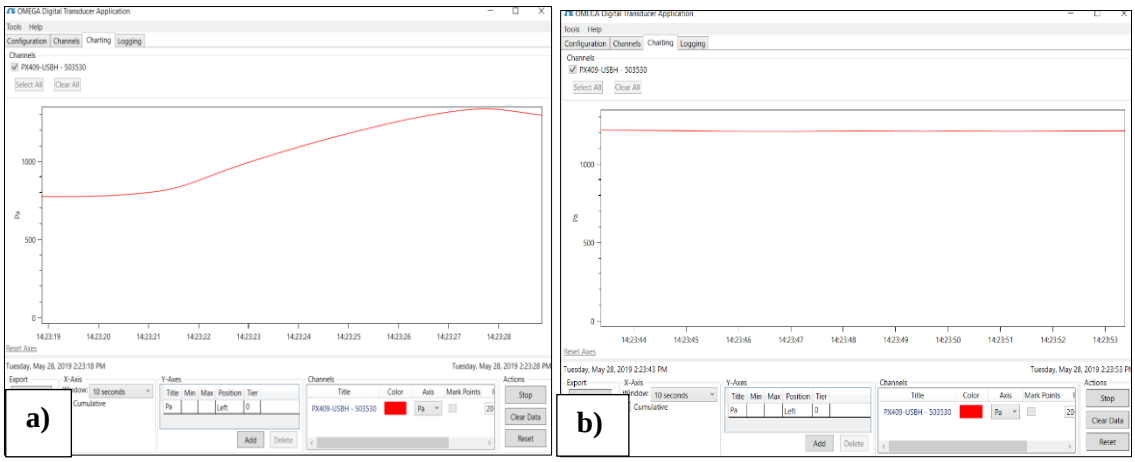

Figure 4. Omega software for chart recording and data logging. a) curve demonstrating the change in pressure or velocity induced by pump's frequency change; b) Steady flow

In practical duct/channel flow the wall shear stress (τ_w) can be related to the head loss due to the friction through the channel. Using a simple momentum balance of turbulent flow in the channel, the relationship for wall shear stress may be given by (6:

$$\tau_w = -\frac{H}{2}\left(\frac{dp}{dx}\right) \tag{6}$$

Where H is the channel height, $\frac{dp}{dx}$ is streamwise pressure gradient. Estimation of the wall shear stress is crucial as it is used to calculate the important friction velocity scale, u_τ given in (7.

$$u_\tau = \sqrt{\frac{\tau_w}{\rho}} \tag{7}$$

The skin friction coefficient C_f is determined by normalizing the wall shear stress with the kinetic energy of the bulk flow:

$$C_f = \frac{\tau_w}{\frac{1}{2}\rho {U_m}^2} \tag{8}$$

Here, ρ is the density of a fluid and U_m is the bulk or mean velocity in the channel.
As mentioned above, channel flow can never be truly two-dimensional unless the AR is infinite, a fact which implies an overestimation of center wall shear stress. The error in calculation of τ_w must depend on AR, since it is this parameter that specifies the extent of two-dimensionality. Such an error term can be included in equation: $\tau_w = \varepsilon \frac{H}{2}\left(\frac{dp}{dx}\right)$. The three-dimensionality factor $\varepsilon(A)$ will be unity provided that the AR is large enough that the flow is nominally two-dimensional near the centre.
The channel height, H can be used as a characteristic length scale to define the Reynolds number ((9).

$$Re_m = \frac{U_m H}{\nu} \tag{9}$$

4. Test panels and their surface characteristics

To generate a reference data set for the smooth surface, test panels made of PVC were used. Alongside, tests were run on various coated panels, all of which were different in type and surface finish. In the experiment, roughness and drag characteristics for coatings were measured and compared. Table 1 presents the details of each coated panel and their roughness. A polyvinyl chloride (PVC) disk acted as a smooth reference surface. Together with the PVC disk, a number of disks were coated with non-biocidal fouling release (FRC) and biocidal antifouling coatings (BAC). Non-biocidal coating samples include: a very durable and tough prototype FRC coating with less fouling release properties (Hard FRC), an epoxy primer (Epoxy), a hybrid coating between Hard FRC and Epoxy types (Hybrid FRC) and a classical FRC coating (FRC) with different application techniques such as the normal and dry spray. Each coating types were applied in duplicate. Maximum peak-to-valley roughness height, *Rt50*, over a 50mm interval was measured using a traditional hull roughness analyzer in order to be able to relate it to ship hull roughness values (Figure 5). Whereas, topographical views for some of the tested panels can be found in Figure 6.

Table 1. Tested coated panels

Test panels		***Rt (50)* expressed in microns (µm)**		**Comments**
		Mean	SD	
Control	PVC (polyvinyl chloride)	33	8.0	Smooth reference
	Epoxy normal 1	61	9.6	Epoxy primer
	Epoxy normal 2	60	9.9	
	Epoxy dry 1	65	10.4	
	Epoxy dry 2	58	11.1	
Non-biocidal	Hard FRC normal 1	36	7.7	Higher cross-linked fouling release coating (less fouling release properties than the classical FRC) with higher toughness and durability.
	Hard FRC normal 2	36	6.6	
	Hard FRC dry 1	50	15.2	
	Har FRC dry 2	55	21	
	Hybrid FRC normal 1	62	11.9	Hybrid between Epoxy and Hard FRC types
	Hybrid FRC normal 2	55	11.5	
	Hybrid FRC dry 1	51	8.6	
	Hybrid FRC dry 2	61	14.3	
	FRC normal 1	50	15.3	Classical FRC coating
	FRC normal 2	53	9.4	
	FRC dry 1	27	10.1	
	FRC dry 2	26	5.4	
Biocidal	BAC normal 1	43	7.1	Classical biocidal polishing coating
	BAC normal 2	45	8.7	
	BAC dry 1	84	10	
	BAC dry 2	87	14	

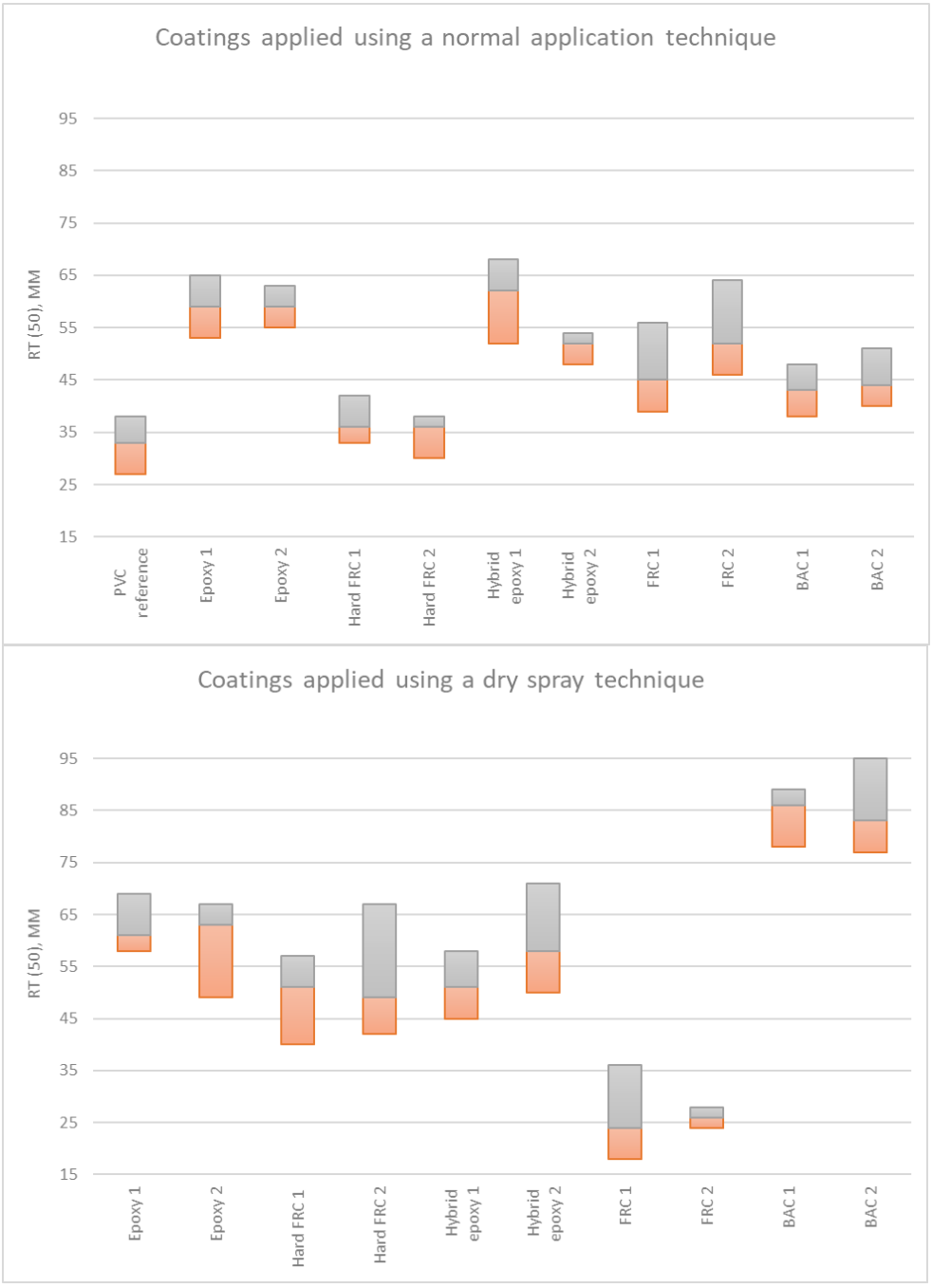

Figure 5. Macro roughness expressed in Rt (50) microns (µm) for reference surface and various types of coatings with different surface finishes

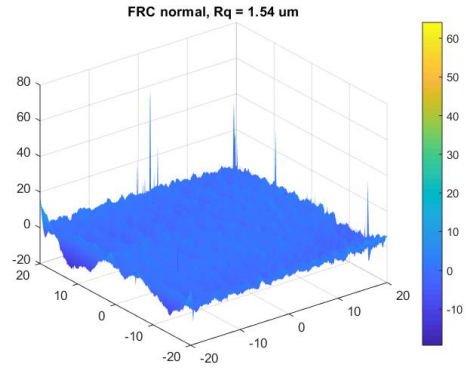
FRC normal, Rq = 1.54 um

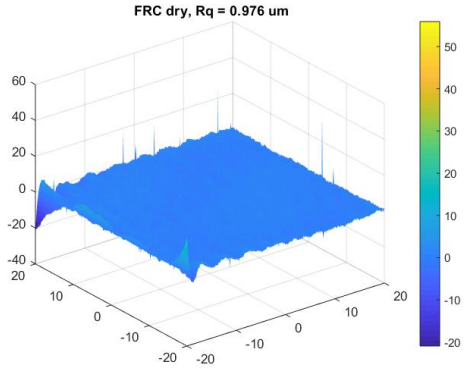
FRC dry, Rq = 0.976 um

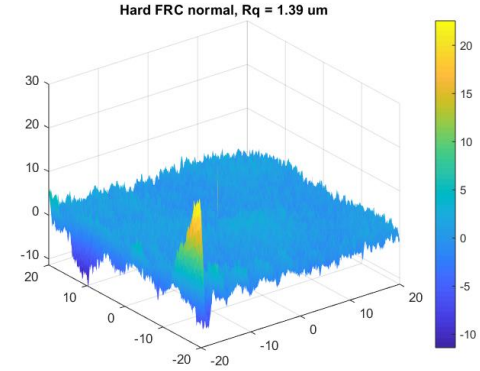
Hard FRC normal, Rq = 1.39 um

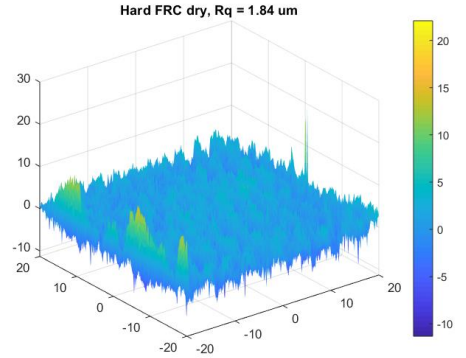
Hard FRC dry, Rq = 1.84 um

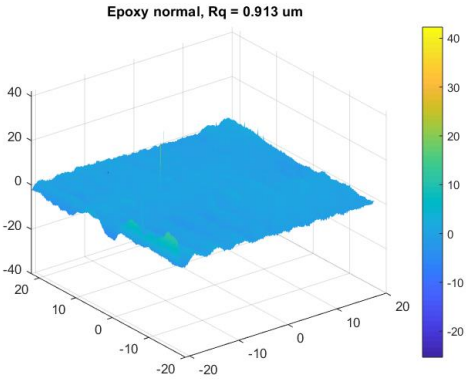
Epoxy normal, Rq = 0.913 um

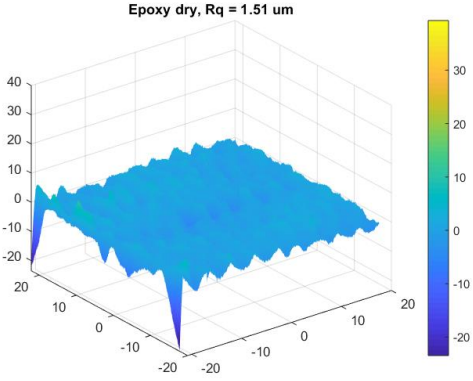
Epoxy dry, Rq = 1.51 um

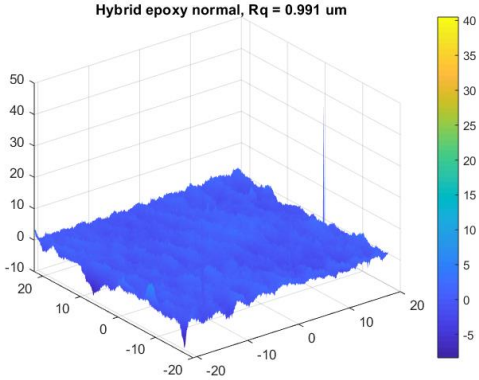
Hybrid epoxy normal, Rq = 0.991 um

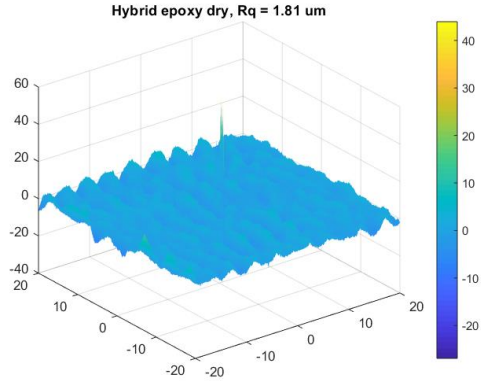
Hybrid epoxy dry, Rq = 1.81 um

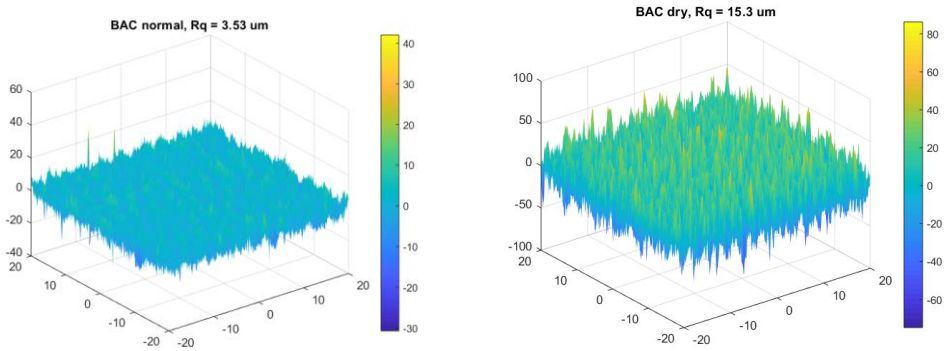

Figure 6. Topographical views of coated test panels. Rq or Root Mean Square (RMS) roughnes is the RMS average of the roughness profile.

Figure 7a and b show examples of BAC and FRCs. Three different types of rough epoxy prime surfaces as shown in Figure 7c, d and e were used for reference measurements. These surfaces were tested by Niebles Atencio and Chernoray [12] in the rotating disk rig to obtain drag (torque), thus roughness functions. As described in Niebles Atencio and Chernoray [12], disks were grinded, cleaned and degreased to enhance adhesion. The coating applications were made by airless spraying of the surfaces to give three levels of roughness. A smooth finish (Figure 7a) roughness is an attempt to simulate an optimal newly built ship or full blast dry docking paint application. Whereas medium level of roughness (Figure 7d) represents a poorly applied coating, and high level of roughness (Figure 7e) represents a severe case of underlying roughness accumulated from many dry dockings. Medium and high level of roughness applications were achieved by deliberate over spraying.

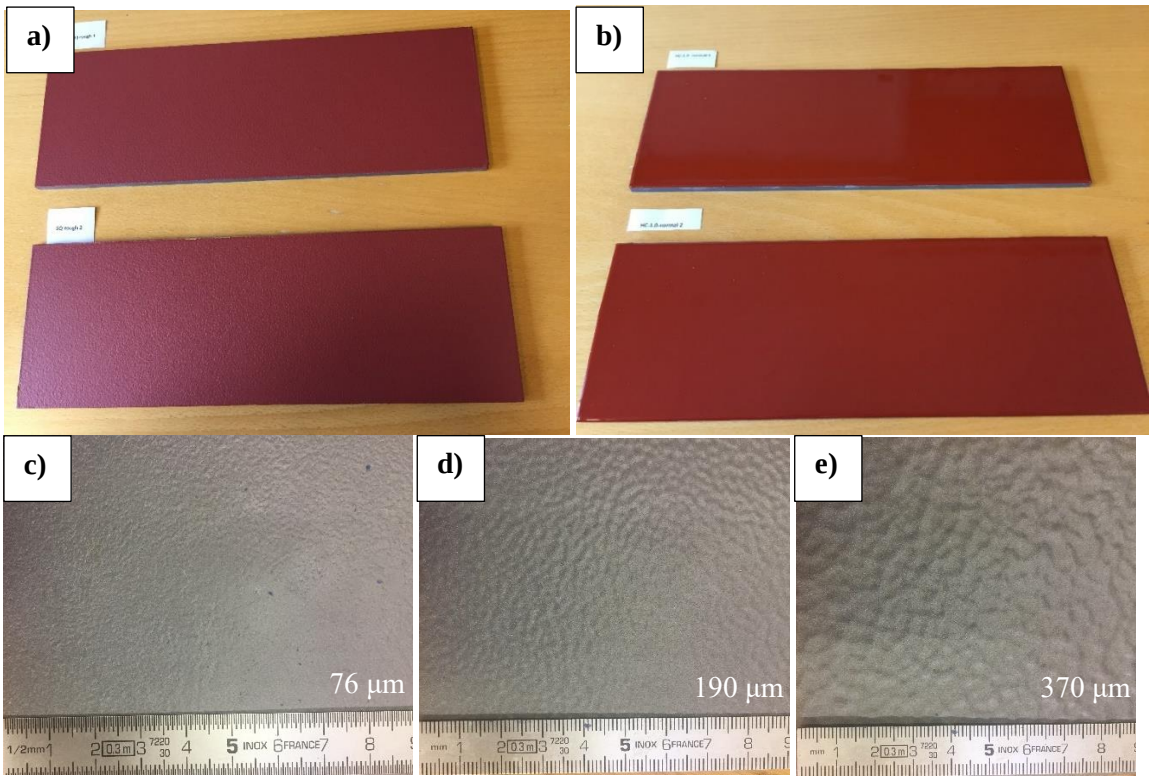

Figure 7. Some examples of tested surfaces; a) Classical BAC; b) FRC type; c) Epoxy primer reference surface with low level of roughness; d) Epoxy primer reference surface with medium level of roughness; e) Epoxy primer reference surface with high level of roughness

5. Results

5.1 Reference measurement

5.1.1 Volumetric flowrate/mean velocity measurements

Pressure readings were taken at the venturi meter. By using the converging section of pipe, the pressure drop was measured to characterize the relationship between motor controller frequency and volumetric flowrate (or mean velocity) through the channel. Motor controller was swept through its entire range of frequencies, from 5Hz to 45Hz. Flowrate corresponding to each pump frequency was deduced from pressure drop using (5. Knowing the flowrate and cross-sectional area of the test section enabled the recalculation of volumetric flowrate at different pump frequencies in terms of mean velocities (U_m) as demonstrated in Figure 8. According to measurement results, the bulk or mean velocity in the testing section ranges from 0.9m/s to 8.8m/s. The maximum differences between the repeat readings were found to be 2-3% at pump frequencies from 10Hz and 30Hz. For the rest pump frequencies uncertainties for U_m were around 1%. As shown, the relationship between U_m and the pump's motor frequencies can be characterized by the linear equation. The trend demonstrates uniform performance of the test rig.

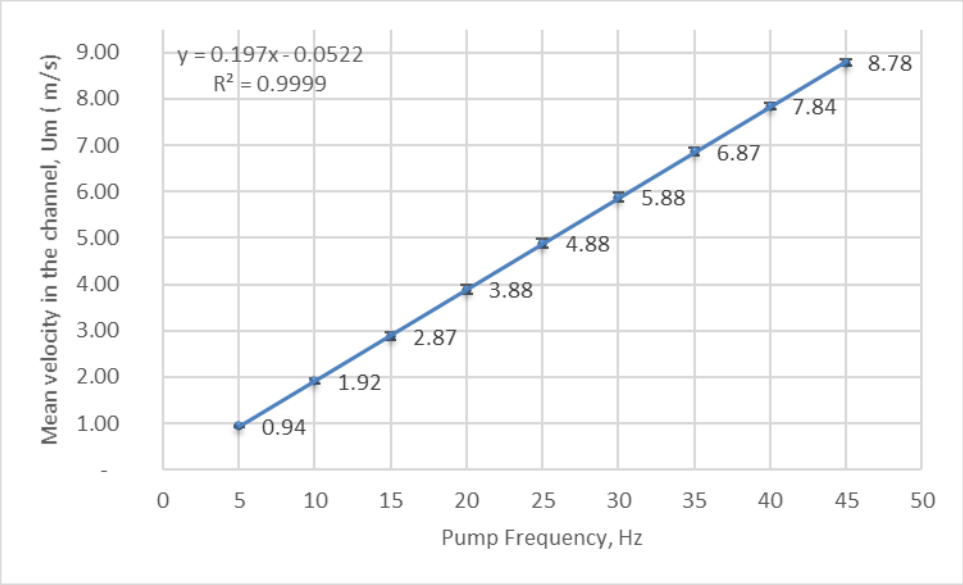

Figure 8. Mean velocity, U_m, as a function of pump's motor frequency

5.1.2 Smooth wall data

Pressure drop was also measured for PMMA smooth panels installed in the testing section, which enabled the estimation of wall shear stresses (and skin friction coefficients) at corresponding velocities. The maximum wall shear stresses are around 150 Pa, which represents a 100m vessel travelling with 27 knots (or 14m/s).

To check the flow development, pressure tappings were installed along the transparent upstream part of the flowcell (see Figure 1a) over a 0.7m of the development section of the flowcell. It is clear from Figure 9, that the static pressure distribution in the flow direction is linear for streamwise distances greater than x/H=40 or 0.4m. This ensures that the flow is developed for all flow velocities before reaching the pressure drop section, where the actual measurements over different panels are taken.

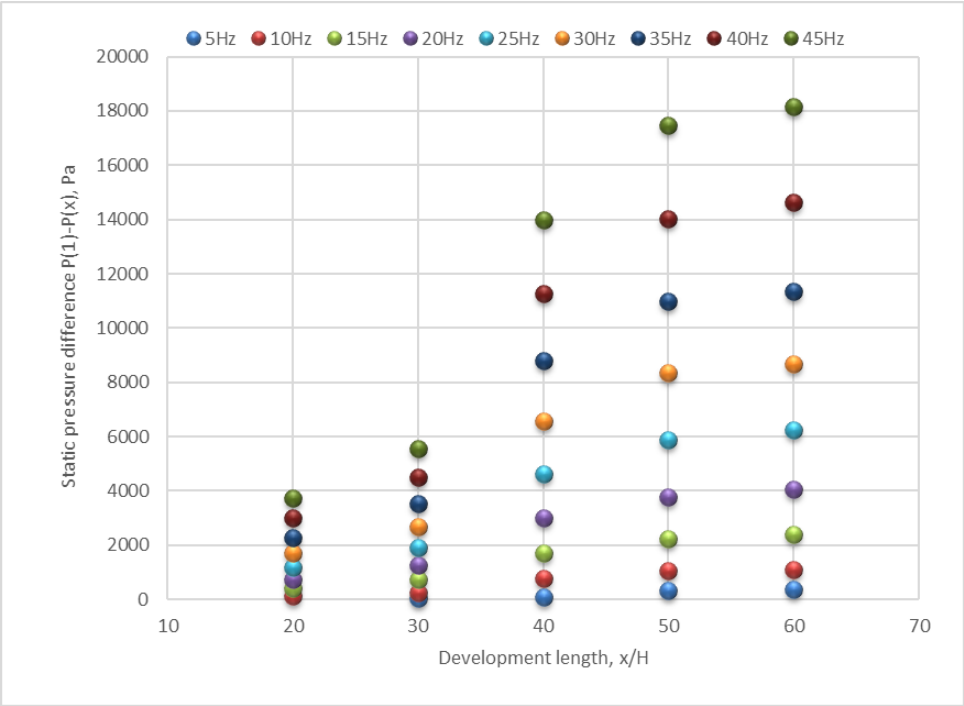

Figure 9. Pressure gradient distribution along the development section at different pump frequencies

Reference data set for the smooth reference was measured and compared to the data in the literature. The data is presented graphically as a plot of skin friction coefficient versus Reynolds number in Figure 10. The correlation from the current study for smooth wall agrees reasonably well for the range 11000 <Re_m< 120000 with the data of Johnston [13] within the experimental uncertainty.

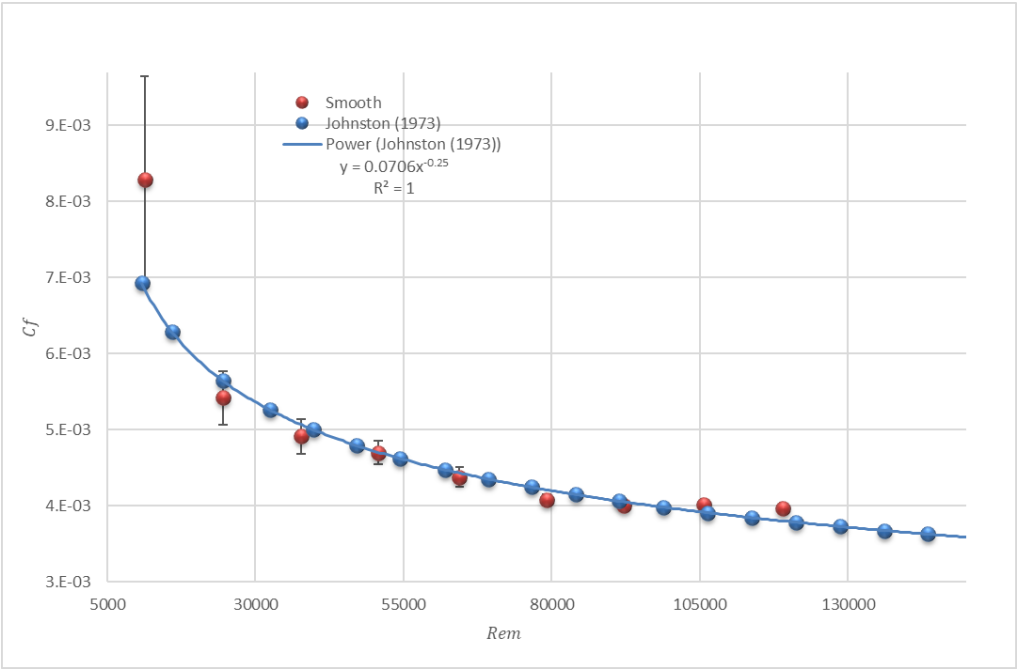

Figure 10. C_f correlation for experimental data for smooth wall

5.1.3 Rough wall data

To present the effect of roughness on epoxy surfaces shown in Figure 7 c, d and e, data in Figure 11 presents the C_f in dependence of Re_m for the flow on downstream part of the test section. With increasing Re_m (Re_m >30000) distinct differences between three levels of roughness can be noticed. Obviously, the epoxy coating with high level of roughness shows the highest C_f throughout the tested Reynolds numbers. Overall, these observations are in agreement with the expected results based on roughness measurements. Interesting to note as well that epoxy coating with low level of roughness is hydraulically smooth until Re_m=20000. Whereas the epoxy surface with medium roughness is hydraulically smooth until Re_m=30000. Epoxy surface with high level of roughness appears to become independent of Reynolds number (or in fully rough regime) from Re_m=80000.

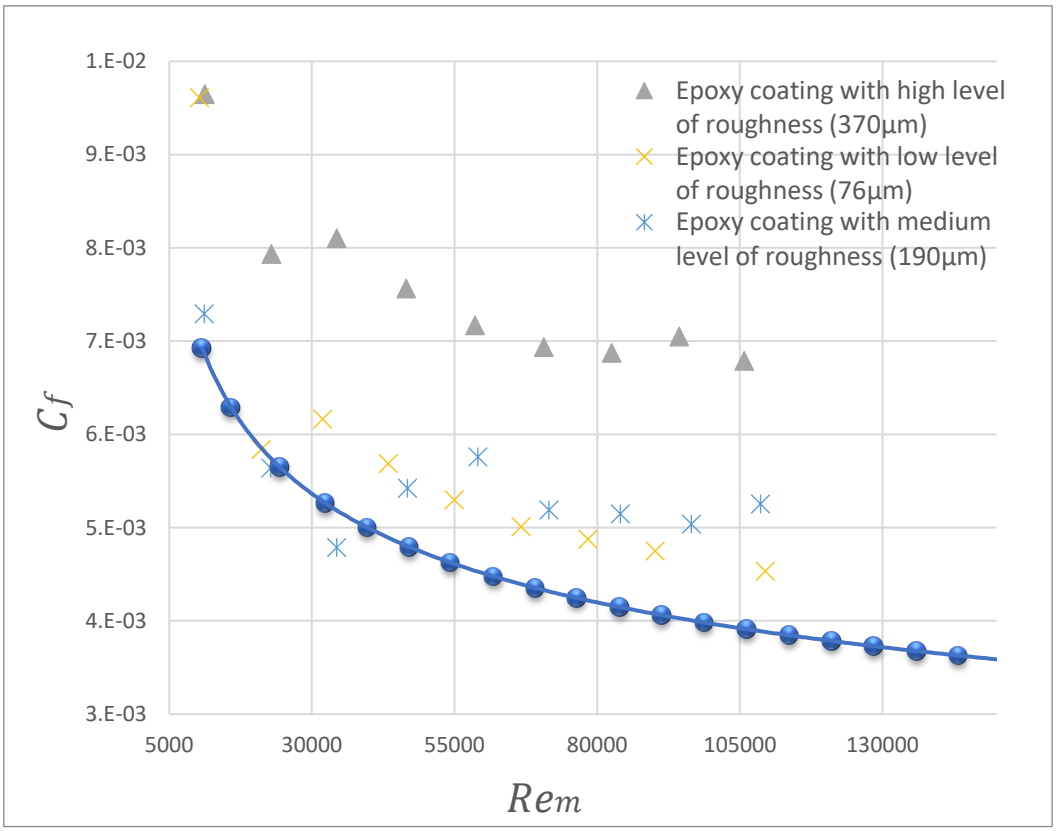

Figure 11. C_f correlation for epoxy coatings with different level of surface roughness

5.2 Coating measurements

The friction coefficient change with Reynolds numbers for various coated surfaces are presented in Figure 12. Starting from Re_m >55000, the distance between the reference smooth curve (shown in solid dotted-blue line) and data for biocidal antifouling coatings (BAC normal, BAC dry) grows until finally the BAC normal and BAC dry coated panels act as additional roughness increasing the C_f. According to topographical views (see Figure 6) and macro-roughness features (see Figure 5), the BAC dry panels were categorized as being the roughest amongst all coated panels followed by BAC normal coated panels.

In general, all other foul-release coatings including the epoxy reference were found to be hydraulically smooth. However, it is difficult to make firm conclusions about the performance grading between each application technique used. Due to the small dimensions of the present flowcell

channel, change of cross-sectional area due to the presence of thin panels (thus bending) is not negligible. Therefore, future panels need to be stiffened to ensure flatness along the panel's length and width.

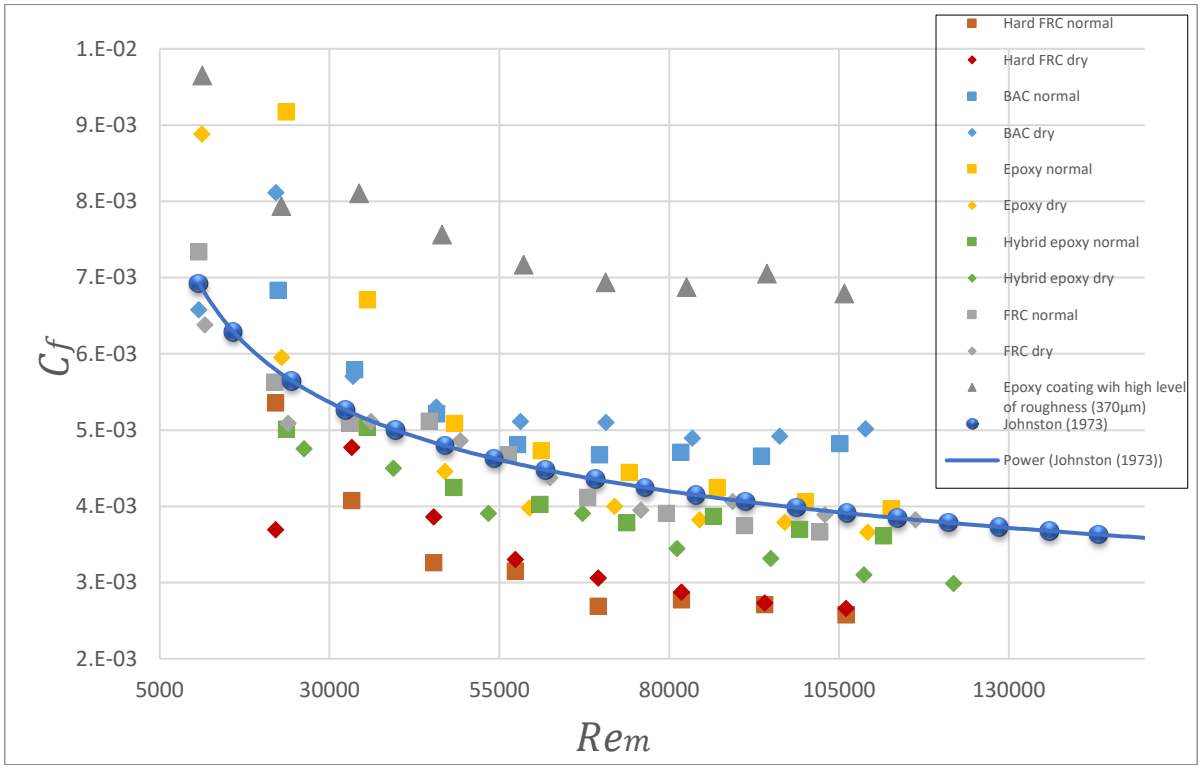

Figure 12. C_f correlation for epoxy coatings with different level of surface roughness

6. Conclusions

The present work deals with skin friction measurements of smooth and coated surfaces with various degrees of surface finishes in newly-built flowcell facility. A channel flow test section with the aspect ratio of AR=8 was chosen to simulate the two-dimensional turbulent flow. The mean velocity and skin friction coefficient are determined indirectly through repeat measures of the pressure drop in the streamwise direction. The first results obtained from flowcell suggest that indirect determination of skin friction from pressure drop measurements is promising.

It appears from the literature review that two dimensional flows are difficult to achieve, since the skin friction coefficient at the core of the channel depends on many factors such as the aspect ratio [3], the length of the development section, the change in channel height and the approach whether the centerline or mean velocity is used for the scaling of the results. Therefore future studies are necessary to correct for AR and to stiffen the base flat panels to accurately represent the skin friction curves.

7. Acknowledgements

Funding support for this study was provided by the Chalmers Area of Advance Transport. We would also like to thank Mr. Mehran Javadi for his unwavering help throughout the experiments.

8. References

1. Durst, F., et al., *Methods to Set Up and Investigate Low Reynolds Number, Fully Developed Turbulent Plane Channel Flows.* Journal of Fluids Engineering, 1998. **120**(3): p. 496-503.
2. Monty, J.P., *Developments in Smooth Wall Turbulent Duct Flows*. 2005, University of Melbourne: Melbourne, Australia. p. 272.
3. Vinuesa, R., et al., *New insight into flow development and two dimensionality of turbulent channel flows.* Experiments in Fluids, 2014. **55**(6): p. 1759.
4. Dean, R.B., *Reynolds Number Dependence of Skin Friction and Other Bulk Flow Variables in Two-Dimensional Rectangular Duct Flow*. Journal of Fluids Engineering, 1978. **100**(2): p. 215-233.
5. Schultz, M.P. and K.A. Flack, *Reynolds-Number Scaling of Turbulent Channel Flow.* Physics of Fluids, 2013. **25**(025104): p. 1-13.
6. Zanoun, E.S., F. Durst, and H. Nagib, *Evaluating The Law Of The Wall In Two-Dimensional Fully Developed Turbulent Channel Flow.* Physics of Fluids, 2003. **15**(10): p. 3079-3089.
7. Hoyas, S. and J. Jiménez Sendín, *Reynolds number effects on the Reynolds-stress budgets in turbulent channels.* Physics of Fluids, 2008. **20**(101511): p. 1-8.
8. Zanoun, E.S., H. Nagib, and F. Durst, *Refined cf Relation for Turbulent Channels and Consequences for High Re Experiments.* Fluid Dynamics Research, 2009. **41**(021405): p. 1-12.
9. Herwig, H. and M. Voigt, *Turbulent entrance flow in a channel: An asymptotic approach.* Lecture Notes in Physics, 1995. **442**: p. 51-58.
10. Reader-Harris, M.J., *Orifice Plates and Venturi Tubes*. Experimental Fluid Mechanics. 2015, NEL, Glasgow, United Kingdom of Great Britain and Northern Ireland Springer.
11. ISO, *ISO 5167-1: Measurement of fluid flow by means of pressure differential devices — Part 1: Orifice plates, nozzles and Venturi tubes inserted in circular cross-section conduits running full*, t.I.O.f.S. (ISO), Editor. 1991, the International Organization for Standardization (ISO): Printed in Switzerland. p. 1-10.
12. Niebles Atencio, B. and V. Chernoray, *A resolved RANS CFD approach for drag characterization of antifouling paints.* Ocean Engineering, 2019. **171**: p. 519-532.
13. Johnston, J.P., *The suppression of shear layer turbulence in rotating systems.* ASME J. Fluids Engin, 1973. **95**: p. 229-236.